

ČESKÉ VYSOKÉ UČENÍ TECHNICKÉ V PRAZE

Fakulta jaderná a fyzikálně inženýrská

Katedra fyziky

Obor: Fyzikální inženýrství

Zaměření: Fyzika a technika termojaderné fúze



BAKALÁŘSKÁ PRÁCE

Samonavigace laserových svazků na termonukleární pelety s
využitím fázově konjugujících zrcadel vytvořených pomocí
stimulovaného Brillouinova rozptylu

Self-navigation of laser drivers on thermonuclear pellets using
phase conjugating mirrors generated by stimulated Brillouin
scattering

Vypracoval: Lukáš Matěna
Vedoucí práce: doc. Ing. Milan Kálal, CSc.
Rok: 2013

(místo téhle stránky přijde zadání)

Čestné prohlášení

Prohlašuji na tomto místě, že jsem předloženou práci vypracoval samostatně a že jsem uvedl veškerou použitou literaturu.

Nemám závažný důvod proti užití tohoto školního díla ve smyslu §60 Zákona č. 121/2000 Sb., o právu autorském, o právech souvisejících s právem autorským a o změně některých zákonů (autorský zákon).

V Praze dne 7. ledna 2013

.....
Lukáš Matěna

Poděkování

Rád bych na tomto místě poděkoval svému vedoucímu doc. Ing. Milanu Kálalovi, CSc. za jeho vstřícnost, ochotu a přátelský přístup při konzultování této práce. Dále bych rád poděkoval svým rodičům, bez jejichž podpory by tato práce nikdy nemohla vzniknout.

Lukáš Matěna

Název práce:

Samonavigace laserových svazků na termonukleární pelety s využitím fázově konjugujících zrcadel vytvořených pomocí stimulovaného Brillouinova rozptylu

Autor: Lukáš Matěna
Obor: Fyzikální inženýrství
Zaměření: Fyzika a technika termojaderné fúze
Druh práce: Bakalářská práce
Vedoucí práce: doc. Ing. Milan Kálal, CSc.
Katedra fyzikální elektroniky, Fakulta jaderná a fyzikálně inženýrská,
České vysoké učení technické v Praze

Abstrakt: Po krátkém úvodu do problematiky jaderné fúze se práce zabývá zkoumáním navržené metody samonavigace laserových svazků na letící peletu s palivem pro inerciální fúzi. Metoda spočívá v ozáření pelety nízkoenergetickým laserovým zářením, které je po odrazu zesíleno, odráží se na fázově konjugujícím zrcadle, je dále zesíleno, konvertováno na vyšší harmonickou a pomocí speciálně navržených pasivních optických prvků je, zcela automaticky a s patřičnou přesností, navedeno zpět na terč. Tento přístup by měl výrazně usnadnit zaměření svazku, v porovnání s aktivním zaměřováním pelety. Hlavním cílem práce bylo zjištění základních charakteristik odraženého záření po superpozici světla z více ozařujících svazků a celkové zhodnocení použitelnosti navrhované metody. Základní parametry byly zjištěny, k posouzení účelnosti celé metody je nicméně třeba pokračovat ve výzkumu.

Klíčová slova: inerciální fúze s přímým zapálením, fázově konjugující zrcadlo, implozní symetrie, navigace laserových svazků

Title:

Self-navigation of laser drivers on thermonuclear pellets using phase conjugating mirrors generated by stimulated Brillouin scattering

Author: Lukáš Matěna

Abstract: After a short introduction into nuclear fusion, a proposed method of self-navigation of laser drivers on a moving fuel pellet is introduced. The method comprises of illuminating the pellet by low energy laser pulse, which is reflected off the target, amplified, reflected on phase-conjugating mirror, amplified further, converted to higher harmonic and by means of specially designed passive optical elements is automatically focused back onto the target. This approach should significantly ease the process of navigation, when compared to active aiming. The main goal of the thesis was to find out basic characteristics of the reflected light after superposition from many illuminating beams and overall evaluation of practical feasibility of the proposed method. The characteristics were found, but further research needs to be done in order to make a final judgement over the method.

Keywords: direct-drive inertial fusion, phase-conjugating mirror, implosion symmetry, navigation of laser drivers

Contents

1	Introduction to nuclear fusion	8
1.1	Nuclear fusion	8
1.2	D-T fusion reaction	9
1.3	Lawson criterion	10
1.4	Magnetic confinement	10
1.5	Inertial confinement	11
2	Self-navigation of laser beams	13
2.1	Basic description	13
2.1.1	Requirements and basic parameters	13
2.1.2	Principle of operation	14
2.1.3	Laser channel design	15
2.2	Proof of concept	16
2.3	Issues to be solved	16
2.3.1	Unconverted first harmonic removal	17
2.3.2	Target reflection ability	18
2.3.3	Parameters of reflected illuminating light	18
3	Reflection of one beam on the target	19
3.1	Geometry and basic assumptions	19
3.2	Numerical model	20
3.2.1	Description	20
3.2.2	Calculating the point of incidence	21
3.2.3	Aiming optimization	22
3.2.4	Phase structure calculation	23
3.2.5	Polarization and amplitude structure calculation	25
3.3	Wavefront shape	28
3.4	Intensity distribution	30
3.5	Phase structure	31
3.6	Polarization structure	33
3.7	Amplitude structure	33

3.7.1	Linear polarization	33
3.7.2	Circular polarization	34
4	Multiple beams reflection	35
4.1	Distribution of laser windows	35
4.2	Superposition	36
4.3	Results	38
4.3.1	Amplitude structure	38
4.3.2	Phase structure	40
4.3.3	Dependence of average amplitude on the number of beams	41
5	Conclusion	42
5.1	Parameters of collected light	42
5.2	Future development	42

Chapter 1

Introduction to nuclear fusion

Note: This chapter serves as really very basic introduction to nuclear fusion, and does not contain any information that is not widely known in the fusion community. Everyone familiar with basic concepts of thermonuclear fusion in inertial confinement can skip this chapter without worries of skipping something they do not already know.

1.1 Nuclear fusion

Nuclear fusion is a process which involves two nuclei joining together to form a heavier nucleus. There are many fusion reactions possible, but those which release significant amount of energy are of particular interest. Fusion reactions are powering the Sun and all other stars, which shows there is high potential of harnessing power. Building a power plant based on nuclear fusion reactions would mean a great step forward for the whole mankind, as it would be very clean energy source with many advantages over both fossil fuel power sources and fission nuclear reactors. The main advantages would be

- virtually indepletable fuel source
- inherent safety
- very small amount of radioactive waste compared to fission reactors

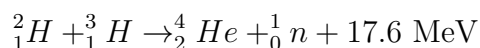
Because the nuclei are positively charged, they repel each other by Coulomb force, and bringing them close enough for strong nuclear force to prevail requires high energy. If the nuclei are to fuse, they first need to overcome this so-called Coulomb barrier. The higher the charge of the nuclei, the higher the Coulomb barrier.

Accelerating a nucleus and letting it hit a target nucleus is possible and functional concept, however, only very few of the accelerated nuclei actually fuse. Most of them dissipate their energy by scattering in the target material. This idea is used in devices called fusors, which are convenient as a source of high-energy neutrons, but building an efficient power plant based on this principle seems impossible.

The most promising method of overcoming the Coulomb barrier is called thermonuclear fusion. It involves heating the fuel to very high temperatures of the order of hundreds of millions of Kelvins. The fuel would necessarily be in the state of plasma, a mixture of free ions and electrons which would move rapidly and occasionally collide with each other. Because the particle kinetic energy is very high at such high temperatures, some of the collisions would make the nuclei overcome the Coulomb barrier and enable them to fuse. Scattering is now not a problem, because the energy is not lost, but stays in the plasma (in an ideal case, when losses are neglected).

1.2 D-T fusion reaction

The most important criterion for choosing a nuclear reaction suitable for a future fusion reactor is its cross section dependence on energy. This cross section should be high for as low energies as possible, which means focusing mainly on reactions involving lighter nuclei, which have smaller charge and therefore lower Coulomb barrier. The most suitable reaction from this point of view is deuterium-tritium reaction. Its cross section has by far the highest maximum from all potential reactions, when achievable energies are considered.



It also has two drawbacks. The energy is released as kinetic energy of the products, majority being carried away by the neutron. The reactor would therefore be subject to high flux of high energy neutrons, which puts high requirements on materials it is made of. Secondly, tritium is not naturally abundant and would have to be bred by some other nuclear reaction. Reactions of lithium with the fast fusion neutron can be used for this purpose, but the need to do so increases complexity of the device and requires further research.

However, other reactions either have too high Coulomb barrier, and would require very high plasma temperatures, or the fuel is unlikely to be available in sufficient quantities (such is for instance the case of reactions involving helium-3 nuclei). It is not impossible that sometimes in the future other

reactions than D-T will be used, but at the present even the D-T reaction, which seems the easiest to achieve, is a challenge.

1.3 Lawson criterion

Because energy losses are not negligible in real thermonuclear plasma, it has to be continuously heated so that the temperature does not drop and the fusion reactions do not cease. In D-T fusion, part of the output energy is carried by an alpha particle, which is easily absorbed in the plasma itself, and therefore contributes to the heating. Under certain circumstances this energy alone could suffice to cover energy losses, which would start self-sustaining thermonuclear burn, and any outer heating system could be turned off. This state is referred to as *ignition*. It should also be noted, that runaway reaction is not possible, because as temperature rises, cross section of D-T fusion decreases. Ignited plasma could burn in a stable state.

Condition for ignition of D-T fusion is known as Lawson criterion:

$$n\tau_E \geq f(T)$$

where n denotes density and τ_E energy confinement time (which is a measure of rate at which energy is lost from the plasma). $f(T)$ is a function of temperature with a minimum at about 25 keV. Providing that the temperature is given, Lawson criterion basically says that the quicker the energy is lost from the plasma, the more the plasma has to be compressed in order to achieve ignition.

1.4 Magnetic confinement

The temperatures needed to allow fusion reactions to occur are in the order of hundreds of millions of Kelvins, which is high above what any known material could withstand. The thermonuclear plasma cannot be allowed to physically touch any part of the reactor, because it would immediately cool down. Many devices based on so-called magnetic confinement are being built and tested. They rely on high magnetic field that, if configured properly, keeps the plasma from touching the walls of the reactor. The most promising family of such devices are *tokamaks*. A tokamak is a doughnut-shaped vacuum vessel with strong toroidal field coils. Charged particles of the plasma are forced to follow toroidal field lines, and therefore cannot leave the plasma. However, because of various effects this configuration of magnetic field is not sufficient to confine the plasma, and another magnetic field has to be added. This field

is called *poloidal* magnetic field, and is made by inducing electric current in the plasma. Strong toroidal field and current induced in the plasma are what defines tokamak and distinguishes it from other configurations. Other systems have to be added to heat up the plasma to sufficient temperatures. The topic is complex and will not be described here in detail.

Ignition has not yet been achieved in tokamak configuration, but high achieved values of $n\tau_E$ show that it is likely to be technically possible, and further research in this field is in progress, with large tokamak ITER currently being built. Plasma density in tokamaks is generally very low, and in order to meet Lawson criterion, long energy confinement time has to be achieved.

1.5 Inertial confinement

Another way of meeting Lawson criterion is to use high density plasma with short energy confinement time. A possible way how to achieve this is rapidly heating a small amount of fuel, so that Lawson criterion is met and significant portion of the fuel is ignited and burned, before the system has time to expand and cool down. This idea is known as inertial confinement fusion, because it is only inertia that keeps the system from expanding. The energy would obviously be released in pulses, power could not be produced continuously.

In currently considered configuration, the fuel is stored in a small hollow spherical pellet, which contains D-T gas and a layer of D-T ice. The outer layer is made of plastic. The target has to be cryogenic at very low temperatures. Other configuration would make the compression process ineffective. High power lasers (drivers) can be used to compress the target and heat the resulting plasma.

In order to compress the fuel successfully, the irradiation has to be very precise and isotropic. The system is vulnerable to instabilities, which can compromise the whole process. That is why so-called *indirect drive* scheme was proposed. The target is enclosed in small hollow cylindrical cavity called *hohlraum*, and the lasers irradiate the inner surface of this cavity. Laser energy is converted to X-rays, which then irradiate and compress the target itself. Irradiation is more symmetric if done this way.

Recent situation at the world's largest inertial confinement device, National Ignition Facility, shows that achieving ignition will likely be more difficult than anticipated, due to previously unexpected problems[1]. Indirect drive hohlraums scatter a significant part of the energy away from the target, and the irradiation symmetry is not sufficient. This comes as a disappointment for inertial fusion community.

Ignition has not yet been achieved in this configuration either. Even if

it is achieved eventually, there are many issues to overcome before a power plant is built. Energy released in a single shot is limited by the design of the reactor chamber, and in order to get continuous and high power thermal output, the demands on repetition rate of the drivers are high and cannot be met by present technologies. Ion beams could be used instead of the lasers, but there are other issues with them as well. And even if the repetition rate of the drivers is high enough, the targets would have to be changed very rapidly, which makes another issue.

Another experimental device for inertial fusion is so-called *z-pinch*. High current is driven through a cylindrical plasma, and resulting magnetic field compresses and heats it. The largest of these called Z machine is located in Sandia National Laboratory. Very high temperatures have been achieved in these devices, and research in this field continues.

Chapter 2

Self-navigation of laser beams

As shown in previous chapter, there are still many problems to be solved in inertial confinement fusion development, before a functional inertial fusion power plant can be built. An ignition has not yet been achieved, not even on stationary targets with indirect drive. Assuming that it will be in a few years time, there will be other issues on the list. A stationary target is not suitable to be used in a power plant – setting it in a proper position would take time, and because the energy output of each explosion is limited, overall power output would be too small. Therefore, one possible solution is to inject the target into the reaction chamber, and irradiate it by the laser beams as it flies. This might highly improve the repetition rate, but also brings the question of how to aim the lasers on the moving target. Tracking the target and aim at it¹ is an option, but might prove to be too difficult. However, an alternative approach was proposed[4][5][6][9]. An approach that might possibly require no active aiming at all (although some passive tracking of the target will still be needed).

2.1 Basic description

2.1.1 Requirements and basic parameters

The whole idea assumes that a way to ignite thermonuclear pellet by lasers in direct drive scheme has been already found and that a laser repetition rate is high enough, and deals with the problem of how to aim at this pellet, moving very quickly in the reaction chamber. Let's first estimate basic parameters of the whole process. A spherical target 4 mm in diameter is injected into

¹by either moving some focusing optics, or by adjusting refractive index of suitably chosen optical element (Kerr effect)

spherical reaction chamber 10 m in diameter. In order to achieve isotropic irradiation, the target has to be delivered into a virtual sphere 5 mm in diameter in the center of the chamber, and the aiming precision needs to be about 20 μm . Providing that one explosion has an energy of 1 GJ, and that the total power output required is 5 GW (so that the net electricity output is comparable to conventional fission reactors), the frequency would have to be about 5 Hz. The injection velocity would have to be in the order of hundreds of meters per second. It will obviously be difficult to achieve the precision needed under these circumstances. Some sort of tracking and optics adjustments is necessary, because it is impossible to predict the position of the pellet precisely enough based solely on its injection speed and direction, due to collisions of the target with debris from previous explosions.

2.1.2 Principle of operation

The alternative approach suggests that it might be possible to obtain the information about the target position by illuminating it by low-energy lasers just before it reaches the center of reaction chamber. The reflected light could be collected by optics, amplified, reflected on phase-conjugating mirror to preserve its wavefront shape, and sent back to the target to ignite it. Because the reflected light is used to do the final high energy irradiation, the low energy illuminating lasers have to be evenly distributed and illuminate the target from all directions. Even though the position of the target during the illumination and irradiation stage would not be the same, the displacement between these stages would hardly change from shot to shot. If the target is injected at 100 ms^{-1} and the optical path the light needs to pass through the amplifiers is 400 m, the displacement would be 130 μm , which is comparable to the required precision margin mentioned above. However, it is still higher than that, and the light cannot be sent exactly where it was reflected from. Instead, it has to deviate from the original trajectory, so that it hits the target in its new position. A way to do this was proposed, and will be described later.

Because the exact position for the low energy illumination is not known, some tracking of the target will be necessary, in order to make sure that the target is in a position suitable for illumination. However, using laser beams wide enough to cover the whole target during acceptable delivery could remove the need for active aiming. Whether this is actually possible depends mainly on the way the injection mechanism is designed, and whether it is able to deliver every target with nearly the same velocity. If, for instance, the direction of the injection is stable enough, it is possible to measure only the speed of the target in order to time the illumination accordingly, and no

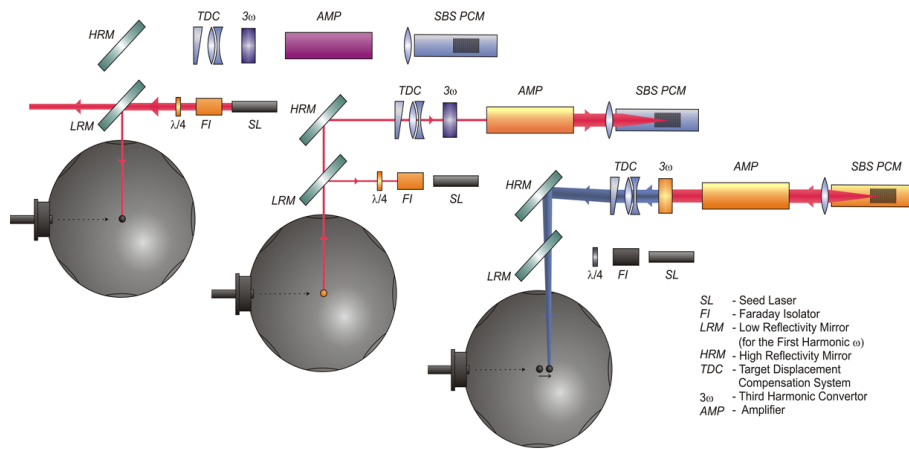


Figure 2.1: A scheme of one laser channel in three different stages of operation[4]

active aiming would be needed. The requirements on the injection mechanism are very high. In case the target is delivered too far off-center, irradiation symmetry is compromised, because one side of the target will be irradiated significantly earlier than the other.

2.1.3 Laser channel design

An important question is how to deal with the position difference between illumination and irradiation stage. A way must be found to deflect the amplified light from its original trajectory. This displacement compensation system has to be custom made for every single laser window, because the deflection angle depends on the window position. An elegant way based on higher harmonic conversion was proposed². The principle is shown in Fig. 2.1.

When the target reaches the middle of the chamber, it is illuminated by seeding laser. The reflected light is collected, passes through higher harmonic conversion crystal (unchanged due to its low energy), is amplified, reflected on phase conjugating mirror and further amplified. On its second pass through the conversion crystal it is subject to higher harmonic conversion and then it enters the target displacement system. It consists of suitably chosen optical element with such refractive index dependence, that the refraction of higher harmonic produces desired angle deflection. Therefore, when the amplified light enters the reaction chamber again, it does not follow its original path. If the target displacement system is adjusted properly, the high energy light

²If Nd:YAG lasers are used, the higher harmonic conversion has to be implemented anyway, because the Nd:YAG wavelength is not suitable for compression of the target.

would hit the target almost exactly in the right spot, and with the same wavefront shape that was produced during the reflection on the target.

2.2 Proof of concept

In order to show that the principle described above works, two experiments have been conducted[6]. The scheme of the more advanced one is shown in Fig. 2.2. The low energy laser light is reflected on a steel ball, passes through the same optical elements as described above, and it is focused on a CCD camera on its way back. Two distinct spots captured by the camera show that the third harmonic converted light indeed followed different trajectory than the unconverted part.

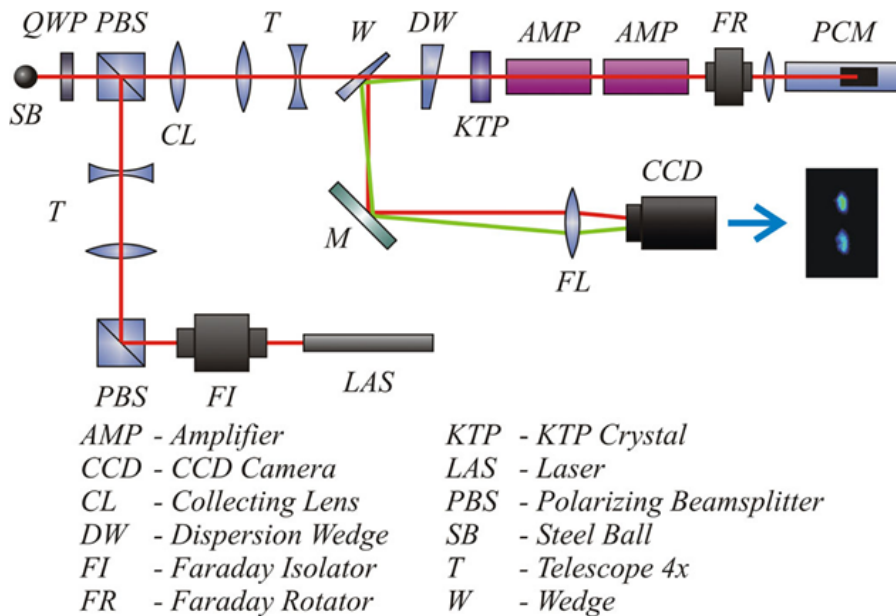


Figure 2.2: Experimental setup[6]

2.3 Issues to be solved

Although the description given so far may sound easy, there are some problems that need to be addressed and solved.

2.3.1 Unconverted first harmonic removal

The higher harmonic conversion is never perfect. Tens of percent of original light intensity may pass through the conversion crystal unconverted. Because it is the first harmonic, the target displacement system would not deflect it where it is supposed to, and the light would likely hit the target off-center, compromising isotropic irradiation, thus preventing ignition. This light must therefore not be allowed to enter the reaction chamber, and must be filtered out and dumped. Whatever optical element is used to do the task, it must allow the first harmonic through on its first pass.

This could be done by Faraday rotator. The idea is shown in Fig. 2.3. Faraday rotator is in between two polarizers that have relative orientation of $\frac{\pi}{4}$. The light collected from the target is polarized by the first polarizer. Then the plane of polarization is rotated by $\frac{\pi}{4}$, and the light passes through the second polarizer. When the mixture of first and higher harmonic returns, it first passes through the second polarizer to ensure the polarization is linear, and then enters the rotator again. Unconverted first harmonic is rotated by $\frac{\pi}{4}$ again, so the first polarizer will not let it enter the chamber. The higher harmonic is rotated by such an angle, that the plane of polarization matches the orientation of the first polarizer, and the light passes through.

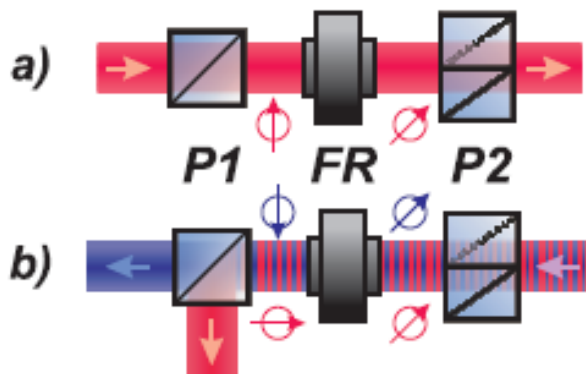


Figure 2.3: Unconverted first harmonic removal[6]

Verdet constants that determine the angle of rotation in Faraday rotator depend on wavelength, so this behaviour of the rotator can be achieved by carefully choosing material for the rotator. If that is not possible, the rotator can be made of two different materials (technically two rotators placed in serie), and the required adjustments can be made by applying different magnetic fields. For further details see [6].

2.3.2 Target reflection ability

The self-navigation would only work if the target reflects enough laser light to be collected and amplified. If the target absorbs too much energy, the scheme will not work, because the targets are delivered at very low temperatures, and premature heating by absorbing the seeding light would compromise compression. That is why calculations were made in order to find out temperature increase as a function of absorbed energy [4]. The calculation shows (see Fig. 2.4) that absorption of 14 mJ of energy means temperature increase of 1 K (providing that 1 ms elapses between illumination and irradiation of the target). This is very important to find out what energy is acceptable for illuminating lasers, and what amplification is necessary afterwards.

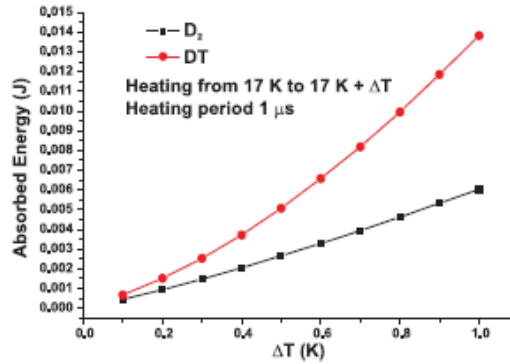


Figure 2.4: Target temperature increase as a function of absorbed energy[4]

It is likely that reflection coefficient of the target will not be sufficient to meet requirements, and some sort of thin reflective coating might be necessary. This will however need further examination.

2.3.3 Parameters of reflected illuminating light

As mentioned above, the target would have to be illuminated by many laser beams from all directions, in order to ensure sufficient symmetry of subsequent high energy irradiation. The collected light would therefore consist of reflected light from many beams, which would superimpose. A crucial question therefore arises: will the characteristics of the collected light be suitable enough for amplification and PCM reflection? And if so, can the light be sent back to the target in a shape capable of symmetric irradiation? This is the main purpose of this thesis. To find out structure of the phase and the amplitude of the reflected light after all illuminating beams superimpose on a chosen window.

Chapter 3

Reflection of one beam on the target

3.1 Geometry and basic assumptions

Geometry in which the problem will be studied is similar to NIF parameters. The target chamber is spherical $R_1=10$ m in diameter, the target is a sphere $2a=4$ mm in diameter. Every window is square with a side length of $2r=400$ mm. The window is placed twice as far from the center than is the chamber radius ($R_2=2R_1$). The chamber wall in actual reactor configuration will be subject to high neutron flux, and enough room needs to be reserved for cooling systems and biological shielding. That is why only a narrow channel for collecting the reflected light was used, and all the optical elements were placed farther. The position of a window in the chamber will be described by two coordinates φ, ϑ . Their meaning is shown in Fig. 3.1. The calculations are however performed in cartesian coordinates.

For the sake of simplicity, the target is assumed to be spherical and positioned exactly in the middle of the chamber. It is also assumed to be 100 % reflective, so any absorption mentioned in Section 2.3.2 is not considered. If the self-navigation concept will appear to be possible in this simple scenario, deviations from these assumptions will have to be taken into consideration as well.

The laser beam is square (although it is not particularly important), aimed at the center of the chamber, and is wide enough to illuminate the whole target. It is therefore not possible to place a window opposite to another one – any light that does not hit the target would enter the opposite window, which is not acceptable. Even if a narrow beam was used (narrower than the target diameter), it is probably not a good idea. For safety reasons

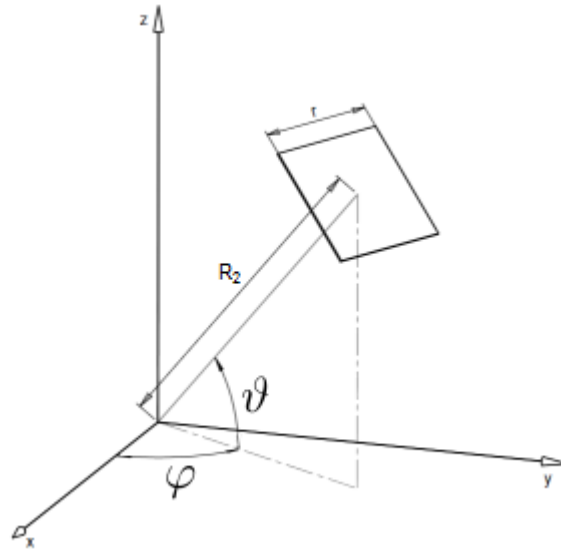


Figure 3.1: Chamber geometry and meaning of coordinates φ, ϑ

it would be wise to place the windows in such a way that no laser light from any window can be fired into another one. Proper window positioning will be dealt with in the next chapter.

The window is not considered flat for the calculation, but instead is curved so that it follows curvature of a sphere. The justification is as follows. Behind the window there has to be lens to make the beam parallel. This lens would convert spherical wavefronts to plane ones, so parameters of the light on the curved window should be the same as would be on a plane window after passing through the lens. The benefits of this approach will be shown in section 3.5.

3.2 Numerical model

3.2.1 Description

Because analytical solution would be difficult to find even in this simplified scenario, and mainly because it would be beneficial that the model can be used to analyse the more complicated scenarios later (narrow beam, non-spherical target etc.), a numerical model based on Monte Carlo simulation was used.¹It was implemented in C++ programming language, and *Mersenne*

¹Analytical solution for wavefront shape after the reflection can be found in [2]. However, it cannot be used to calculate all parameters of interest (like polarisation).

twister[7] pseudo-random number generator implemented in Boost 1.51 library was used.

The principle is very simple. A random ray from the beam is selected and followed to the target. If the target is hit, the ray is reflected based on law of reflection and followed to the sphere with windows. If the examined window is hit, all necessary parameters are calculated and saved. This is repeated until enough rays hit the window. The parameters that have to be calculated are path travelled by rays before hitting the window (which is necessary to calculate phase) and amplitude. Amplitude would normally stay the same, but as was noted in Subsection 2.3.1, the beam that enters the optics will pass through a polarizer after it is collected – which will affect amplitude. The calculation of amplitude therefore means calculating polarization of incident light and comparing it with polarizer orientation.

3.2.2 Calculating the point of incidence

The laser beam source is positioned in the direction of x , in the distance of R_1 from the center, its cross section is a square with side length of $2a$. The target is described by ellipsoid equation

$$\frac{(x - s_1)^2}{a^2} + \frac{(y - s_2)^2}{b^2} + \frac{(z - s_3)^2}{c^2} = 1$$

Two random numbers p_1, p_2 describing a ray in the laser beam are generated in the interval $(-a, a)$. The intersection of the ray and the target can be written as

$$A = (s_1 + \sqrt{K}, p_1, p_2)$$

where

$$K = \left(1 - \frac{(p_1 - s_2)^2}{b^2} + \frac{(p_2 - s_3)^2}{c^2} \right) a^2 \quad (3.1)$$

If $K < 0$, the target is missed.

Next step is to find direction of the reflected ray. Simple geometry implies that

$$\vec{k}_2 = \vec{k}_1 - 2 \frac{\vec{k}_1 \cdot \vec{n}}{\vec{n} \cdot \vec{n}} \cdot \vec{n}$$

where \vec{k}_1, \vec{k}_2 are vectors of incident and reflected rays, respectively, and \vec{n} is a vector normal to the target surface at point A . Substituting

$$\vec{k}_1 = (-1, 0, 0) \quad (3.2)$$

$$\vec{n} = (\sqrt{K}, p_1 - s_2, p_2 - s_3) \quad (3.3)$$

and by introducing the constant

$$E = \frac{2\sqrt{K}}{K + (p_1 - s_2)^2 + (p_2 - s_3)^2} \quad (3.4)$$

one gets

$$\vec{k}_2 = \left(E\sqrt{K} - 1, E(p_1 - s_2), E(p_2 - s_3) \right) \quad (3.5)$$

As noted above, the window is sphere-shaped, so the incidence point on the window can be found as an intersection of a sphere of radius R_2 and a line described by vector \vec{k}_2 which passes through the point of incidence on the target A . Let the intersection be (X, Y, Z) .

The next step is to rotate the point in such a way that the center of the window, if rotated, would lie on x -axis. The reason to do this is because the parameters that one is interested in will be studied as functions of the position on the window, i.e. in 2D. Considering the meaning of coordinates φ, ϑ (Fig. 3.1), it means rotating the point by $-\varphi$ around z -axis and by $-\vartheta$ around y -axis. After the rotation the x coordinate will be discarded, and the remaining two will describe position on the window. The transformed point can be written as

$$\begin{pmatrix} X' \\ Y' \\ Z' \end{pmatrix} = \begin{pmatrix} \cos \varphi \cos \vartheta & \sin \varphi \cos \vartheta & \sin \vartheta \\ -\sin \varphi & \cos \varphi & 0 \\ -\cos \varphi \sin \vartheta & -\sin \varphi \sin \vartheta & \cos \vartheta \end{pmatrix} \begin{pmatrix} X \\ Y \\ Z \end{pmatrix} \quad (3.6)$$

All that remains is to determine whether the point lies in the examined window. This clearly happens when $|Y'| \leq r$, $|Z'| \leq r$ and $X' > 0$. Calculating the path the light travelled is then a straightforward task.

The position on the window can be described by only two coordinates (X' for a successful hit is always equal to R_2 , and can be discarded as already mentioned). In the rest of the thesis there will be various quantities examined as functions of the position on the window. Letters x and y are going to be used in such cases to avoid confusion, even though in the above Y' and Z' is used.

3.2.3 Aiming optimization

When the rays are randomly selected, only very few hit the selected window due to the configuration geometry. Vast majority of them either does not hit the target at all, or ends up somewhere on the inner wall. It is therefore

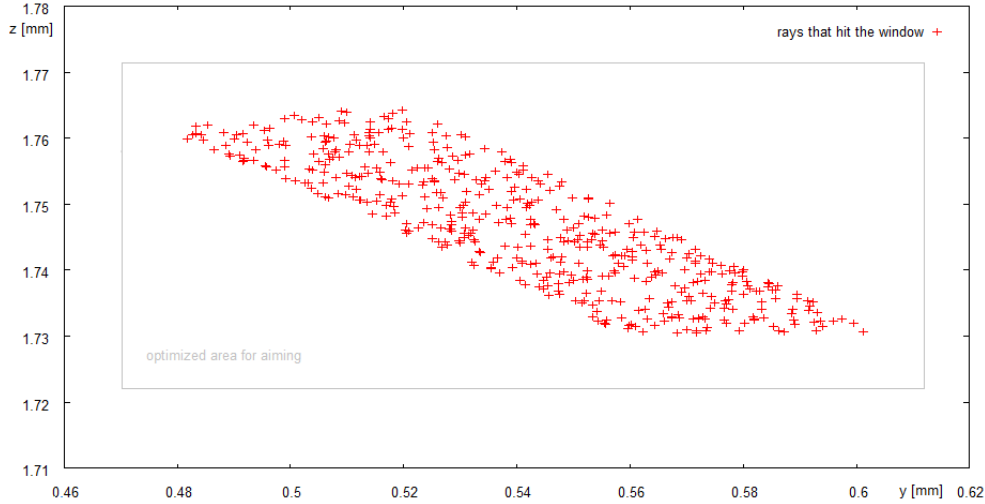


Figure 3.2: Beam cross-section: rays that hit the window at $\varphi = \frac{9}{10}\pi$, $\vartheta = \frac{1}{4}\pi$ and optimized aiming area

helpful to find a way to pick rays in some more sophisticated manner, in order to speed up the simulation. A simple, yet effective way was found and implemented by the author.

At the beginning the rays are indeed picked randomly, and whenever a ray hits the window, the position in the beam in $y - z$ plane where it originated from is checked. After 500 hits accumulate, the minimal and maximal ray positions in both y and z directions are found and used to narrow the effective beam area in a following manner. These four numbers define a rectangle, which is scaled by a factor of 1.2 while the position of its center is not changed. The rest of the rays is again picked randomly, but only in this rectangle. It is shown in Fig. 3.2 for a window position $\varphi = \frac{9}{10}\pi$, $\vartheta = \frac{1}{4}\pi$ (the ray position is $\varphi = 0$, $\vartheta = 0$, as it will be throughout this chapter).

As can be seen, the area of this rectangle is much smaller than the area of the original beam (which is 4×4 mm), which significantly reduces time needed to do the calculations. It is possible to hit the target with thousands of rays in much shorter time. 10000 hits appear to be enough to do all calculations that will be described, and that is the number that was used.

3.2.4 Phase structure calculation

As was demonstrated in subsection 3.2.2, it is very easy to calculate path the light travelled for every beam that hits the window. However, working this

way means we only know the travelled path in the points that were actually hit – and these are essentially randomly scattered. It is necessary to divide the window by a regular grid, and calculate the travelled path (and any other quantity that might be needed) on this grid.

When the window is curved (as was described in Section 3.1), the travelled path of the scattered points on the window can be described by a plane for nearly all window positions. However, the points do not fit exactly on this plane, and due to the wavelength of the light (1064 nm), the phase is very sensitive to path difference. It can be shown that fitting the travelled path by this single plane will not provide necessary precision.

A different algorithm is used instead. As mentioned above, the goal now is to find approximate travelled path on a regular grid, using points scattered in between grid points. This is achieved by going through the grid one point after another, finding few (6 are used) scattered points that lie closest to the current grid point. After they are found, a plane is fitted through them by least squares method, which produces a function of a form $path(x, y)$, where x and y are coordinates describing position on the window (as described in subsection 3.2.2). This function approximates the travelled path in the vicinity of the current grid point, and therefore can be used to find the travelled path there. By running the simulation multiple times and comparing the values in the grid points it appears that an error that results from this approximation is much less than 1 nm, which is acceptable for phase calculation.

When the travelled path d in the grid points is known, calculating the phase itself is easy. It is given by²

$$\beta = \frac{2\pi d}{\lambda}$$

This phase is then recalculated so that it is the interval $\langle -\pi, \pi \rangle$. $atan2$ function is used – special $atan$ function that uses sine and cosine values of an angle separately, and can therefore determine the quadrant the angle is in. The final formula for phase is

$$\alpha = atan2\left(\frac{\sin \beta}{\cos \beta}\right) \quad (3.7)$$

One last cosmetic alteration of phase will be performed. Phase calculated from the above equation will exhibit steps of 2π . It can be helpful to get

²The phase shift on reflection is not accounted for, because it is the same for all rays, and it is the change of phase on the window that we are interested in, not the specific value.

rid of these, to make the graphs easier to read. To accomplish this, it is possible to try adding or subtracting whole number multiples of 2π to the calculated phase, as this does not make any real difference. The algorithm consists of walking through the grid one row after another, finding the average phase of the grid point left of and above the current grid point (when walking left to right, top to bottom, i.e. the points are already processed) and adding/subtracting such whole number multiple of 2π to the current point phase, that the resulting value is as close to the average as possible. Where there is only one already processed point available next to the current point (first row and column), no average is calculated and only one reference point is considered. The first point of the grid is obviously not changed at all. The result of this process will be shown in section 3.5.

3.2.5 Polarization and amplitude structure calculation

Let's now assume that the beam is linearly polarized. First it is necessary to describe the direction of polarization (i.e. amplitude of \vec{E}). It is described by an angle $\xi \in \langle 0, \pi \rangle$, where $\xi = 0$ means the light is polarized in z direction, and $\xi = \frac{\pi}{2}$ means polarization in y direction. As was already noted, there is a polarizer the light passes through after its collected. Its direction is described in similar manner by an angle γ , zero angle means the polarization direction is the same as the direction of increasing angle ϑ . In other words, if the window is rotated according to equation (3.6), the polarization description is the same for the beam and the window.

It is necessary to find out the change of polarization when the ray is reflected. The basic principle is as follows. The ray is tracked to the point of reflection, and the polarization vector is split into two perpendicular vectors, perpendicular and parallel to the plane of incidence. According to Fresnel equations and given that the target is 100 % reflective, the former is conserved and the latter maintains its norm. Because the direction of reflected light is calculated from law of reflection, the polarization can be calculated as well.

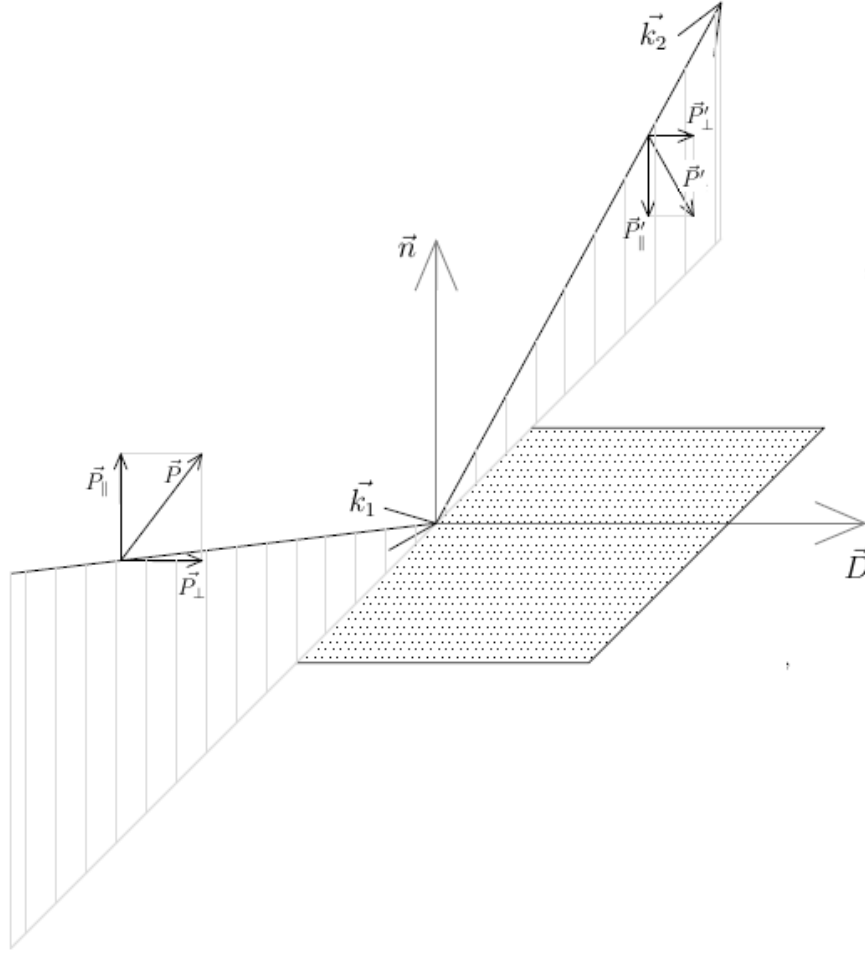


Figure 3.3: Geometry of the problem (schematic – vectors \vec{P} , \vec{P}_\perp , \vec{P}_\parallel , \vec{P}' , \vec{P}'_\perp and \vec{P}'_\parallel are in fact perpendicular to respective rays)

Let \vec{k}_1, \vec{k}_2 be unit vectors of the incident and reflected ray, \vec{n} unit vector normal to the target surface at the point of incidence and $\vec{P} = (0, \sin \xi, \cos \xi)$ the polarization vector. Defining $\vec{D} = \frac{\vec{k}_1 \times \vec{n}}{|\vec{k}_1 \times \vec{n}|}$, one can write

$$\vec{P}_\perp = (\vec{D} \cdot \vec{P}) \vec{D} \quad (3.8)$$

$$\vec{P}_\parallel = \vec{P} - \vec{P}_\perp \quad (3.9)$$

Let $\vec{P}', \vec{P}'_\perp, \vec{P}'_\parallel$ denote the polarization vector after the reflection and its part perpendicular and parallel to the plane of incidence, so that $\vec{P}' = \vec{P}'_\perp + \vec{P}'_\parallel$. As explained above, $\vec{P}'_\perp = \vec{P}_\perp$ and $|\vec{P}'_\parallel| = |\vec{P}_\parallel|$. Because \vec{P}'_\parallel lies in the plane of

incidence and has to be perpendicular to the reflected ray, the polarization vector of the reflected ray can be written as

$$\vec{P}' = \vec{P}_\perp + \vec{P}'_\parallel = \vec{P}_\perp + \delta \cdot |\vec{P}'_\parallel| \cdot (\vec{D} \times \vec{k}_2) \quad (3.10)$$

where δ is either plus or minus one. Its goal is to ensure that vector bases $(\vec{k}_1, \vec{P}_\perp, \vec{P}'_\parallel)$ and $(\vec{k}_2, \vec{P}'_\perp, \vec{P}'_\parallel)$ have opposite orientation – opposite, because the part parallel to the plane of incidence is subject to a phase shift. Looking back at section 3.2.2 and substituting from equations (3.8), (3.2), (3.3), (3.9) and (3.5), one gets these final expressions for the two parts of the polarization vector

$$\vec{P}'_\perp = \frac{(p_2 - s_3) \sin \xi + (s_2 - p_1) \cos \xi}{(p_2 - s_3)^2 + (s_2 - p_1)^2} \cdot \begin{pmatrix} 0 \\ p_2 - s_3 \\ s_2 - p_1 \end{pmatrix} \quad (3.11)$$

$$\vec{P}'_\parallel = \frac{\delta \cdot |\vec{P}'_\parallel|}{\sqrt{(p_2 - s_3)^2 + (s_2 - p_1)^2}} \cdot \begin{pmatrix} E(p_2 - s_3)^2 + E(s_2 - p_1)^2 \\ (s_2 - p_1)(E\sqrt{K} - 1) \\ (p_2 - s_3)(1 - E\sqrt{K}) \end{pmatrix} \quad (3.12)$$

where E and K are given by equations (3.4) and (3.1).

Let $\vec{W}_{pos} = (R_2 \cos \vartheta \cos \varphi, R_2 \cos \vartheta \sin \varphi, R_2 \sin \vartheta)$ be a vector describing position of the examined window. By rotating vector $\vec{P}' + \vec{W}_{pos}$ according to equation (3.6) and discarding the x coordinate (let the new 2D vector be denoted \vec{P}'_l), the polarization of the incident light and the window can be compared. The polarization direction of the polarizer in the window after the rotation is $\vec{P}'_w = (\sin \gamma, \cos \gamma)$, and cosine of the angle between the two (which is equivalent to amplitude attenuation) can be written as $\frac{|\vec{P}'_l \cdot \vec{P}'_w|}{|\vec{P}'_l| |\vec{P}'_w|}$

In summary, a way to find polarization of the ray on the examined window and corresponding amplitude attenuation after the beam passes through polarizer in the window has been found. A similar problem as was described in subsection 3.2.4 arises – it is necessary to calculate these quantities in grid points. Because in this case the changes are not that abrupt, nearest neighbour approximation is used instead of the least squares method.

3.3 Wavefront shape

In order to see how the simulation works, let's first have a look at what the reflected wavefront looks like. In can be easily done if one tracks a ray until certain distance is travelled, and then saves position the light reached. Results for 4 distinct distances travelled is shown in Fig. 3.4.

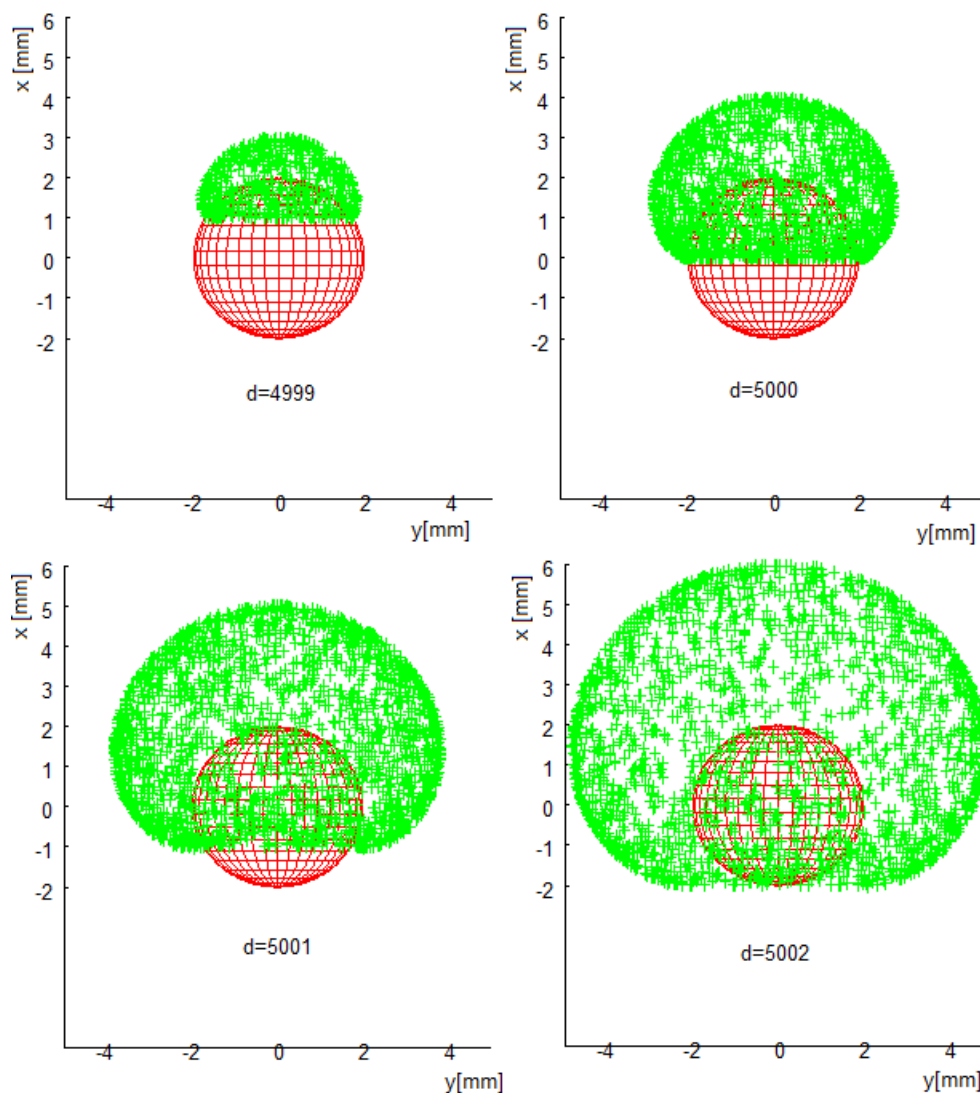


Figure 3.4: Wavefront shape after the reflection, d denotes distance the light has passed (in mm).

Wavefront shapes after reflection off a unit sphere calculated analytically in [2] are shown for comparison (Fig. 3.5). The shadow cast by the sphere is clearly visible in Fig. 3.6 . The same wavefront shapes and the same shadow result from the numerical simulation (shown in Fig. 3.4).

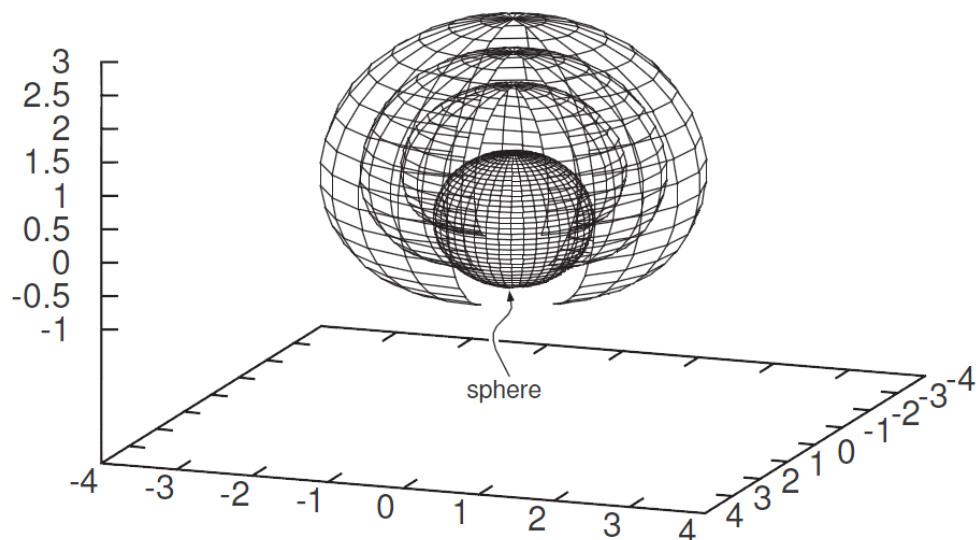


Figure 3.5: Wavefront shapes calculated analytically [2]

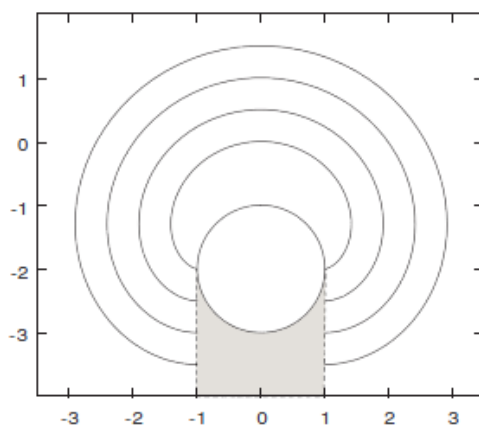


Figure 3.6: Wavefront shapes calculated analytically (side view) [2]

3.4 Intensity distribution

One of the very basic results the simulation can provide is the intensity distribution on the windows. If the target is illuminated by a single beam, the intensity on some windows (one could expect that on those close to the window the beam originated from) might be higher than elsewhere, simply due to geometry. In order to find out, the simulation was run without the optimization process described in subsection 3.2.3, and the polarization was not taken into account as well. Total of 10 million randomly selected rays were tested for every window, and the rays that actually hit the window were counted. Fig. 3.7 shows the ratio of these "successful" rays³.

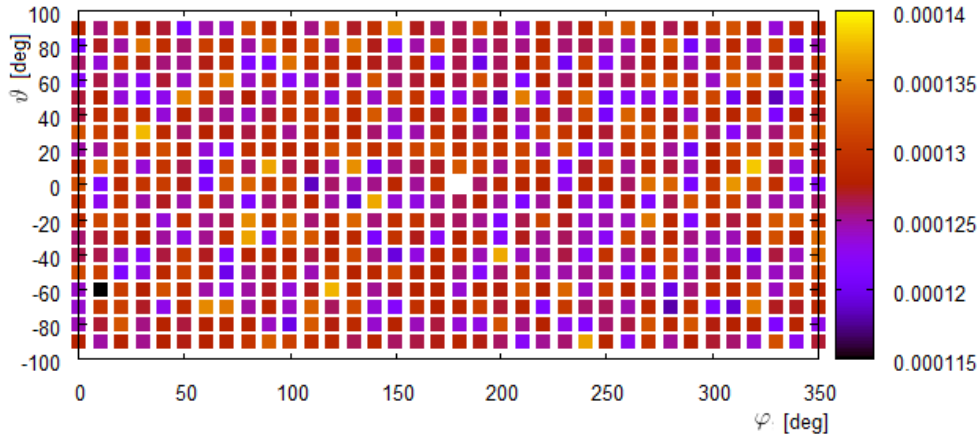


Figure 3.7: Percentage of 10 million rays that hits specified windows

As can be seen, there is no clear dependence of intensity on the window position. The variations of intensity have a character of random noise, which is due to the fact that the intensity calculation is based on random numbers.

If the intensity on the windows is constant, the percentage of rays that hit a specified window should be the same as the ratio of the window area to the surface area of a sphere the windows are positioned on (because every beam is reflected somewhere). This ratio is (the geometry was described in section 3.1)

$$\frac{400^2}{4\pi \cdot 10000^2} \approx 1.27 \cdot 10^{-4}$$

which is consistent with the simulation. The conclusion is that the intensity on the windows is indeed constant, at least as long as the polarization is not taken into account.

³The way the windows are selected would not produce even windows distribution – the window density increases with increasing $|\vartheta|$. This is however not important at this point.

3.5 Phase structure

Examples of phase structure on selected windows can now be presented. The target was again illuminated by a single beam in a position $\varphi = \vartheta = 0$. The phase was calculated on a regular grid 400 by 400 points according to equation (3.7), discontinuities were not removed.

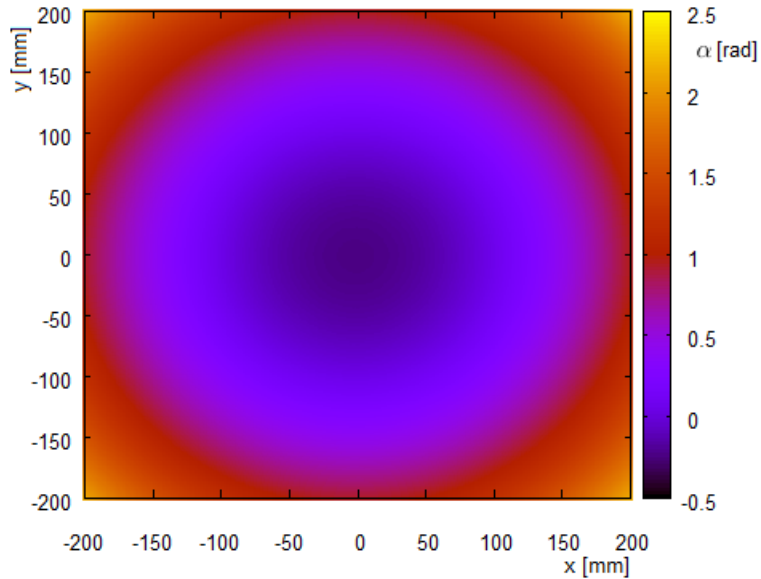


Figure 3.8: Phase structure for the window at $\varphi = \vartheta = 0$

As one would expect, the phase does not change much across the window for back-reflection (Fig. 3.8), and the other window ($\varphi = \vartheta = \frac{\pi}{3}$) phase structure consists of evenly spaced strips (Fig. 3.9). Now the advantage of the fact that the window is sphere-shaped (see the end of section 3.1) can be explained. Had the window been flat, the phase would change rapidly across it and the spacing of the strips would be much smaller than the spacing of the grid, which could render the whole simulation useless.

As promised at the end of section 3.2.4, the effect of there-described discontinuity removing algorithm is shown. Fig. 3.10 shows the same phase structure as Fig. 3.9, except now the 2π discontinuities in phase were removed.

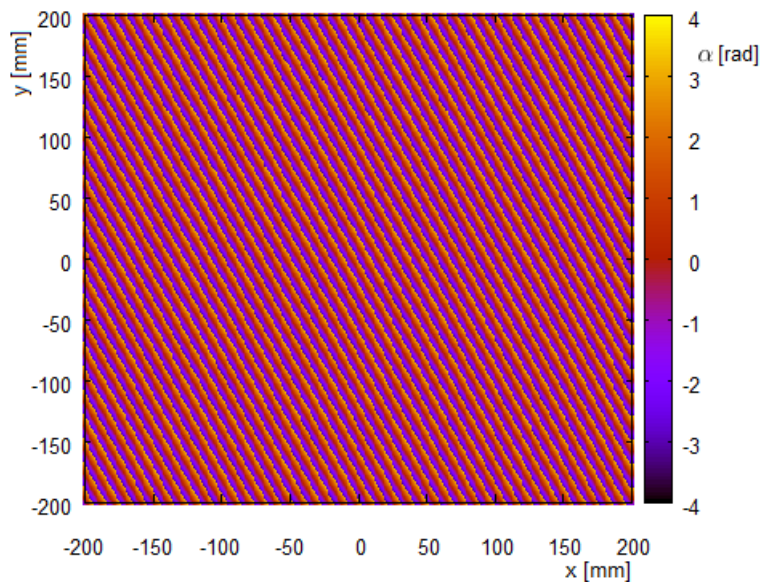


Figure 3.9: Phase structure for the window at $\varphi = \vartheta = \frac{\pi}{3}$, with discontinuities

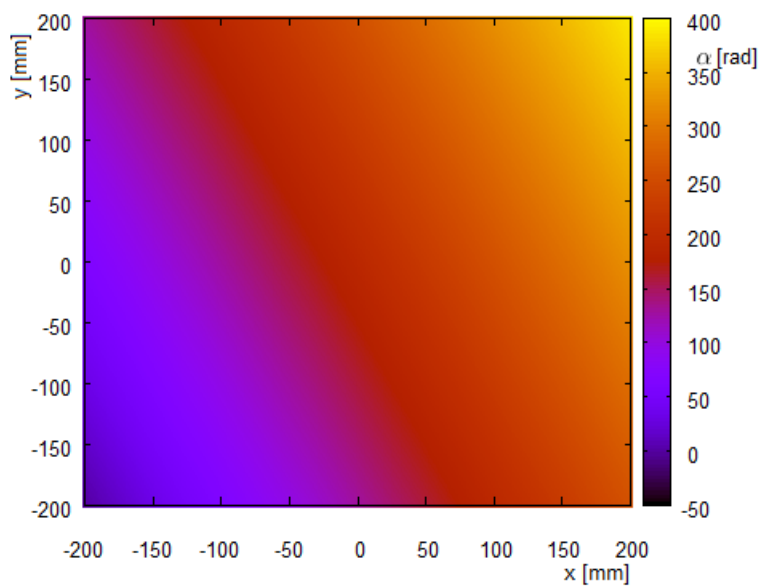


Figure 3.10: Phase structure for the window at $\varphi = \vartheta = \frac{\pi}{3}$, discontinuities removed

3.6 Polarization structure

As for the polarization structure on the window that collects back-reflected light ($\varphi = \vartheta = 0$), there is not much to see. The polarization is the same as the polarization of the original beam across the whole window.

A bit more interesting situation can be seen in Fig. 3.11, which shows polarization on the window positioned at $\varphi = \vartheta = \frac{\pi}{3}$. When the angle ζ equals 0, it means the polarization has the direction of increasing angle ϑ (similar as in section 3.2.5). In the figure this would be vertical direction. The original beam is polarized in z direction, i.e. $\xi = 0$.

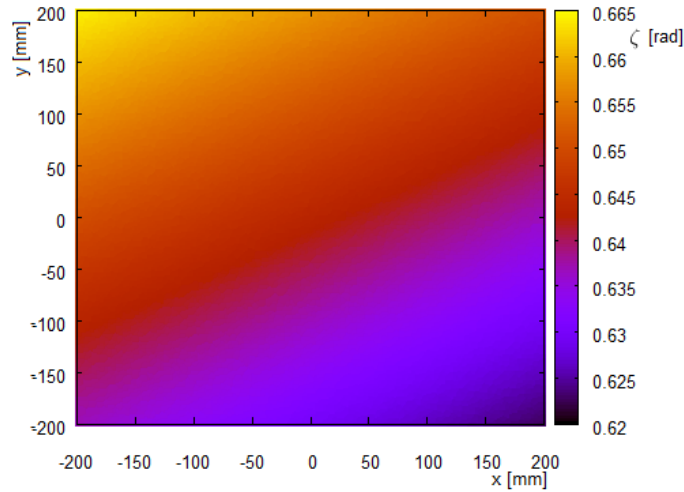


Figure 3.11: Polarization structure for the window at $\varphi = \vartheta = \frac{\pi}{3}$

3.7 Amplitude structure

As already noted in subsection 3.2.1, there is no reason amplitude should be anything but even on all the windows. That is however not the case when the polarizers in the windows are considered.

3.7.1 Linear polarization

If the original beam is linearly polarized, calculating the amplitude after the light passes through the polarizer is simple, and was already mentioned in subsection 3.2.5. All it takes is calculating cosine of the angle between the polarizer and direction of polarization and multiply it by original beam

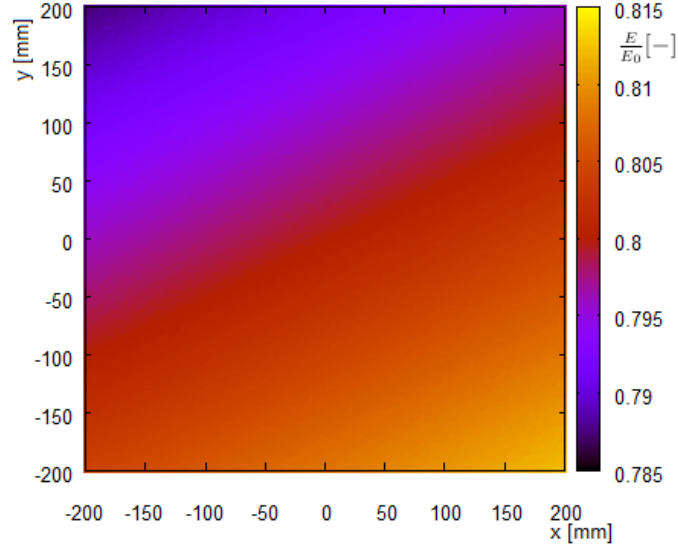


Figure 3.12: Amplitude structure for the window at $\varphi = \vartheta = \frac{\pi}{3}$

amplitude. Let E denote the amplitude after light passes through and E_0 the amplitude of the original beam.

Providing that the window polarizer orientation is $\gamma = 0$, the amplitude structure on the window $\varphi = \vartheta = \frac{\pi}{3}$ is shown in Fig. 3.12. Technically it bears the same amount of information as Fig. 3.11, except the cosine function has been applied.

3.7.2 Circular polarization

As shown above, the need for having the polarizers behind the windows means the amplitude for different windows (after passing through the polarizer) will be different if the original laser beam is linearly polarized, which might imply problems. A simple way to ensure the amplitude is always the same, and yet the light is linearly polarized after it is collected, is using circularly polarized light. Circular polarization is preserved on reflection, and when circularly polarized light meets the polarizer, only the projection into its direction goes through. Due to rapid changes in the beam polarization direction, the mean amplitude behind the polarizer is constant for all the windows. According to Malus law averaged through angles and the fact that intensity is proportional to the square of amplitude, this mean amplitude is

$$E = \frac{1}{\sqrt{2}} E_0 \quad (3.13)$$

Chapter 4

Multiple beams reflection

4.1 Distribution of laser windows

Before a superposition of light from many laser beams can be performed, a way to position arbitrary number of windows in the reactor chamber has to be developed. It is equivalent to distributing points on a unit sphere, which is not as simple task as it may sound. The main goal is to have as symmetric and regular window distribution as possible. Another requirement is that no window is opposite to another one, which was explained in section 3.1. It can be shown that in the geometry that is considered, 2° clearance between the centers of the windows is acceptable.

Regular distribution of points on a sphere can be achieved by using Platonic solids. However, the second requirement is not met in this case, not mentioning that the number of points can not be arbitrarily chosen. Another method must therefore be found.

A simple numerical algorithm was developed. It is actually a simulation of a mechanical system, that is let to evolve in time and results in symmetric distribution of points. The requirement that no points are opposite to each other is not automatically met. However, after the calculation finishes, the resulting distribution is checked, and in case it does not meet the criterion, the calculation is run again. Because the initial positions of the points are random, the result is never exactly the same.

Selected number of points is randomly distributed on a unit sphere. Each point is attached to the sphere by a powerful spring. One end of the spring is fixed to the sphere – it is free to move on the sphere surface, but cannot leave it. Each point is assigned small positive charge, which gradually increases with time. The points therefore begin to repel each other and would fly

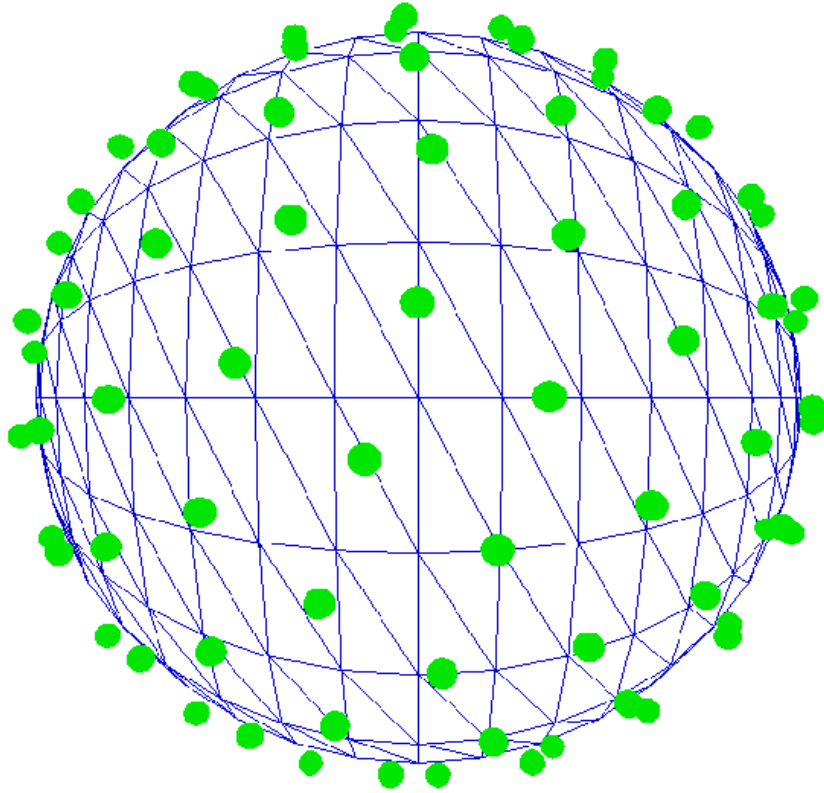


Figure 4.1: Final distribution of 150 points (perspective view, the points on the back side are obscured by the sphere)

to infinity, without the constraints realized by the springs. A friction force proportional to velocity is also introduced.

The system tends to converge to a state of minimal energy, which means maximizing distances between the points. When the points come near stopping, their positions are saved and the simulation terminates. Many distributions made of different number of windows have been generated using this simulation, and will be used for positioning the windows later on.

4.2 Superposition

Everything is now ready to start illuminating the target with more laser beams, and study the characteristics of the light that interferes on a given window. Geometry described in section 3.1 assumes that the beam always illuminates the target from the direction of x axis. However, the choice of the reference frame is arbitrary, and by rotating the whole system conveniently,

any position of both the beam and the window can be simulated. All that is needed is to take a window distribution generated as described above in section 4.1, position a window that the light will be studied on to any of the points, and illuminate the target from every point one by one, while calculating the resulting light characteristics that arise from superposition of the single beams.

Having polarizer in each window is very helpful now, because it ensures that the polarization of the light on a given window will always be the same, regardless of what was the position and polarization of the original beam. This means there is no need to worry about polarization anymore. Calculating the result of superposition of two beams means simply adding two harmonic waves of the same frequency. The calculation will again be performed in the grid points on the window.

The result of such adding is again a harmonic wave of the same frequency, but generally with different phase and amplitude. Let E and α be the amplitude and phase of the resulting wave and $E_1, E_2, \alpha_1, \alpha_2$ amplitudes and phases of the two interfering waves. Then (for details see [3], p. 282)

$$E = \sqrt{E_1^2 + E_2^2 + 2E_1E_2 \cos(\alpha_2 - \alpha_1)} \quad (4.1)$$

$$\tan \alpha = \frac{E_1 \sin \alpha_1 + E_2 \sin \alpha_2}{E_1 \cos \alpha_1 + E_2 \cos \alpha_2} \quad (4.2)$$

Calculating E is straightforward, for calculating α one has to use *atan2* function again (like it was used in subsection 3.2.4) to place the resulting phase to a proper quadrant.

The target is illuminated by the first beam and both amplitude and phase in grid points are saved. Then the second beam is added, and the phase and the amplitude that would result from illumination from this beam only is added to the values from the first beam straightaway, as the grid points are processed. Any number of beams can be added this way.

4.3 Results

All results presented below are for the case of circularly polarized light. Calculating the other case would mean to find some way to choose optimal polarization orientation of the windows, which was not done yet. Results for three different window distributions of 5, 100 and 400 windows will be shown.

4.3.1 Amplitude structure

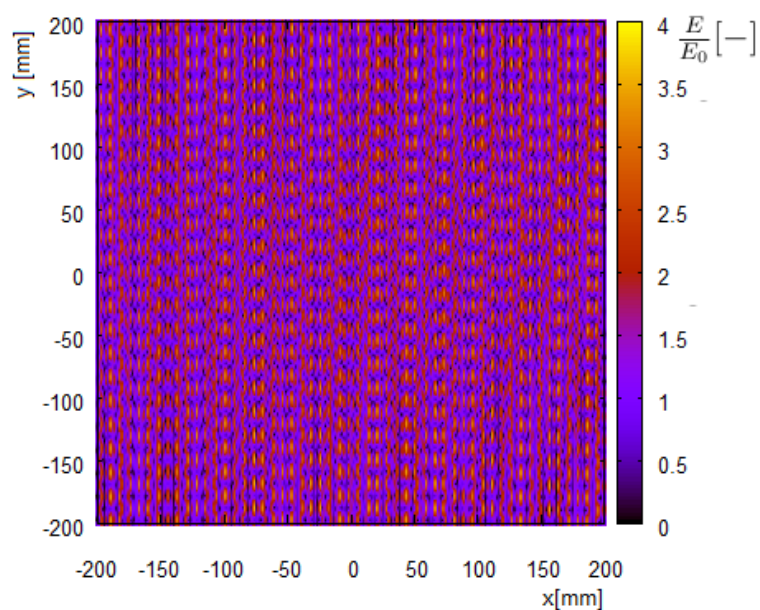


Figure 4.2: Amplitude structure on a window after illuminating with 5 beams

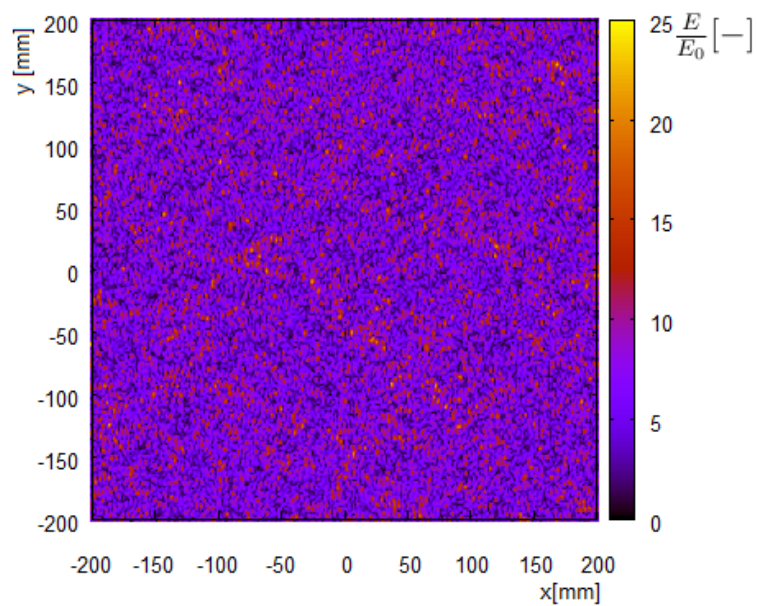


Figure 4.3: Amplitude structure on a window after illuminating with 100 beams

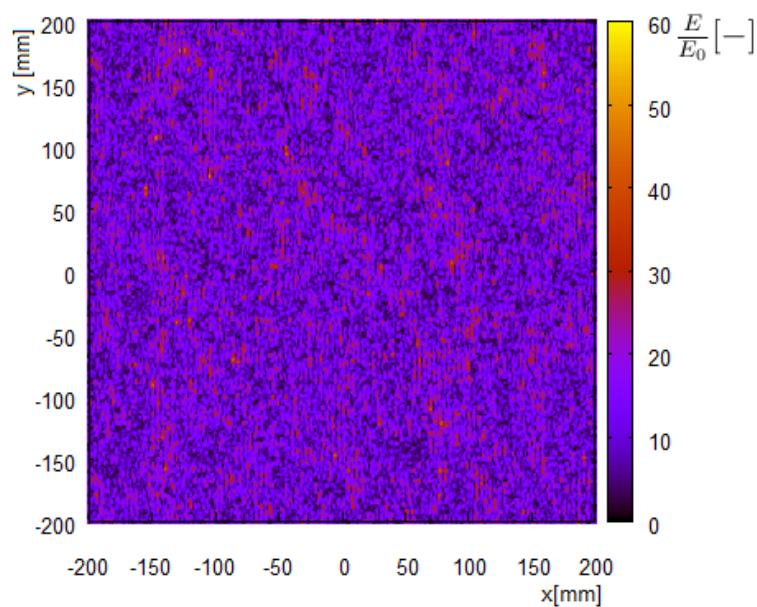


Figure 4.4: Amplitude structure on a window after illuminating with 400 beams

4.3.2 Phase structure

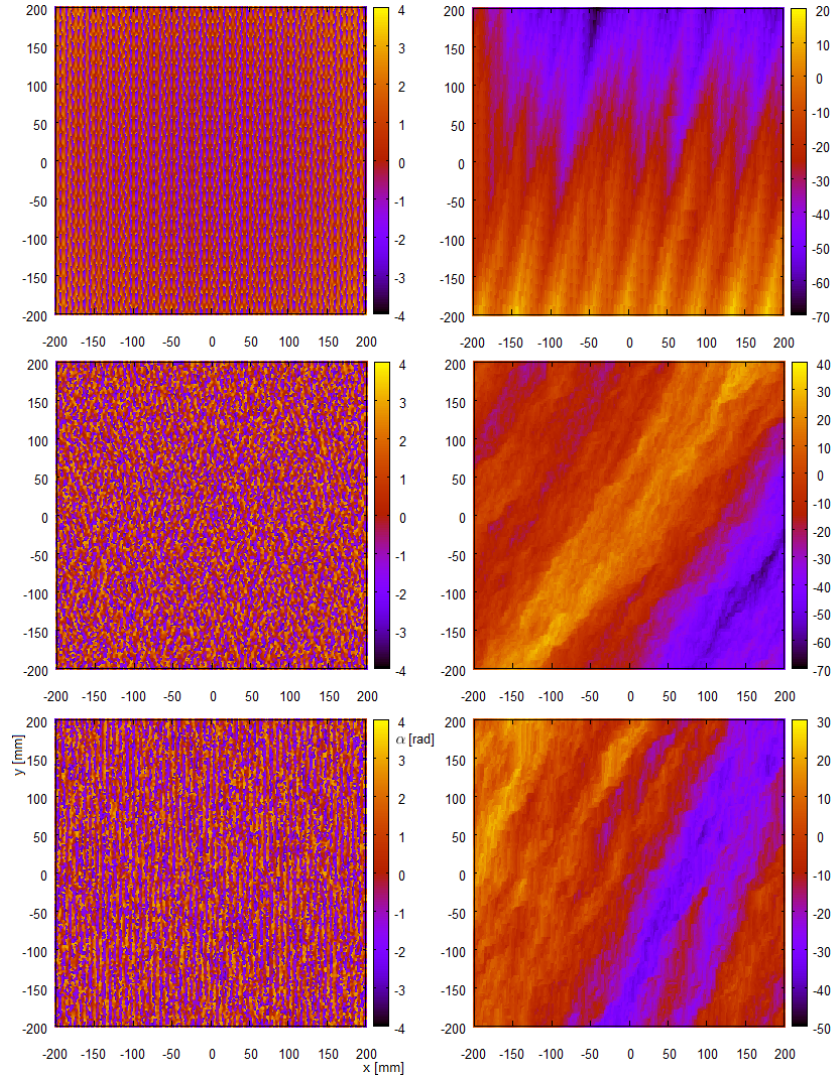


Figure 4.5: Phase structure (both with and without discontinuities) for illuminating from 5, 100 and 400 beams (top to bottom)

All phase structures above are shown both with and without discontinuities (the algorithm for removing them was described in subsection 3.2.4). It should be noted, that when the discontinuities in phase are frequent across the window, the resulting structure after the removal may not look better than original – a better way to remove discontinuities could probably be found. This is however not the goal of this thesis, and the calculations that will be later performed with phase are not affected by whether this process

was done or not. One has to realize that the discontinuities are result of the method used for calculating phase, and do not have any physical meaning.

4.3.3 Dependence of average amplitude on the number of beams

Important questions now arise. What is the average amplitude of the radiation across the window, how do the single grid points differ from this average, and what is the dependence of these values on the number of beams used? To answer this question, the simulation was run many times for many different window distributions, and the resulting amplitude maps were analysed. Each map is discrete (it is made of grid points) so calculating an average amplitude as an average of the grid points values is simple, as well as calculating standard deviation. The result is shown in Fig. 4.6. As can be seen, average amplitude increases as \sqrt{N} and the variation coefficient is always almost exactly the same (independent of N), around 0.52.

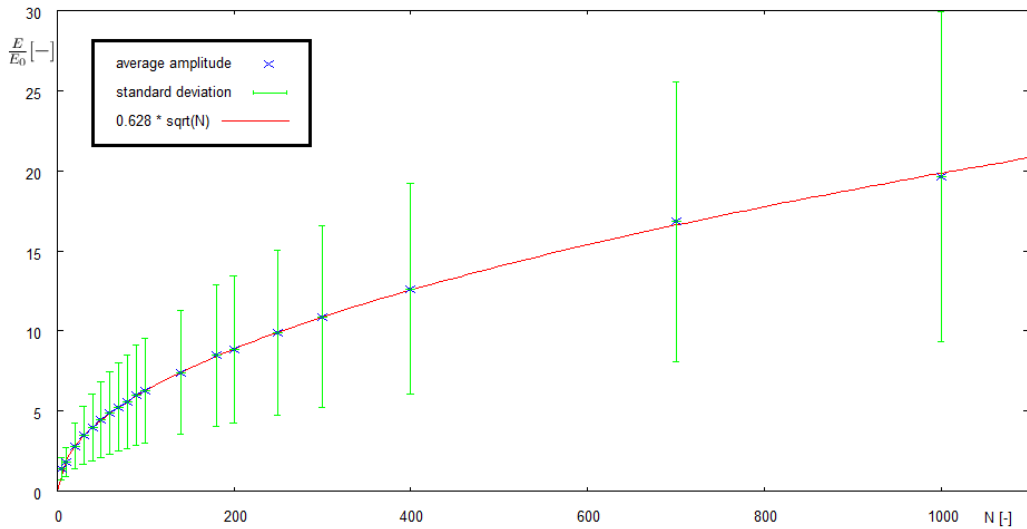


Figure 4.6: Average amplitude and standard deviation for different number of beams

Chapter 5

Conclusion

5.1 Parameters of collected light

As can be seen from section 4.3, amplitude of collected light after superposition changes rapidly across the window, and the variation does not depend on the number of beams used. In order to verify whether proposed self-navigation method can work, further research needs to be done to find out how will the collected light behave in amplifiers, whether the resulting beam will be able to reflect on phase conjugating mirror, and whether the phase and amplitude structure of the light after reflection is good enough for the beam to compress the target. It is likely that the amplitude inhomogenities will pose an issue during these steps, and methods will have to be sought to make the parameters of the laser beam even.

So far only circularly polarized light was considered. In case the light is linearly polarized and the polarizers are conveniently oriented, the resulting amplitude structure might be more stable. If this method does not work, more optical elements might be needed to alter the beam parameters.

5.2 Future development

Even if both amplitude and phase structure were perfectly homogenous, there are other issues that need to be solved. After the beam is collected, it has to travel significant distance through amplifiers. It is however not perfectly parallel, so its structure will change as it travels, and the beam will widen. The changes in beam parameters need to be studied to decide whether they significantly affect the performance. When all this is done and potential problems solved, an ideal number of beams has to be found. The first step might be to establish maximum energy per one beamline.

What also needs to be studied are deviances from the ideal situation that was considered so far. In reality, the target will not be 100 % reflective, it may not be perfectly spherical and smooth, and it will not be precisely in the middle of the target chamber. All of these assumptions have to be broken and the changes of the resulting beam parameters have to be evaluated in order to make a final judgement on whether the self-navigation technique can work in real conditions.

Beside all these issues connected to the self-navigation technique, there is a lot of issues with inertial confinement fusion itself, as already briefly described in the first chapter. The time for self-navigation technique will not come before a direct-drive ignition is achieved in static case and the laser repetition rate is significantly increased, which on the other hand gives time to develop the self-navigation technique further. Tackling the difficulties of inertial fusion itself may or may not be possible, which one has to realize before they become over-optimistic. However, research moves quickly forward and what now seems nearly impossible may become reality in near future. In case a way will be found to ignite the static pellet by lasers, and their repetition rate is increased to a value required for a power plant, it will be needed to deliver the pellets into the reaction chamber and irradiate them as they fly at high frequency. Providing that the injection system will be able to deliver the pellets to the center of the reaction chamber precisely enough, some method of navigating the laser beams onto the target will be needed. The proposed self-navigation technique could be one candidate, and because any other candidate will have its problems as well, it would be wise to develop it so that it is advanced enough when its time comes.

Bibliography

- [1] BRUMFIEL, G. Laser lab shifts focus to warheads. *Nature* 491, 170-171. DOI 10.1038/491170a. Available online at <http://www.nature.com/news/laser-lab-shifts-focus-to-warheads-1.11745> [cited 2 Jan 2013].
- [2] GUILFOYLE, B., KLINGENBERG, W. Reflection of a wave off a surface. *J. Geom.* 84 (2006) 55-72. Available online: <http://arxiv.org/abs/math/0406212v1>. [cited 27 Dec 2012].
- [3] HECHT, Eugene. *Optics*. Addison Wesley, 2002, 4th edition. ISBN 0-321-18878-0.
- [4] KALAL M. et al. Recent Progress Made in the SBS PCM Approach to Self-navigation of Lasers on Direct Drive IFE Targets. *Journal of Fusion Energy*. Springer US. December 2010. Volume 29. Issue 6. 527-531. ISSN 0164-0313. DOI 10.1007/s10894-010-9351-6.
- [5] KALAL M. et al. SBS PCM Technique Applied for Aiming at IFE Pellets: First Tests with Amplifiers and Harmonic Conversion. *Journal of the Korean Physical Society*. Springer US. January 2010. Volume 56. No. 1. 184-189. DOI 10.3938/jkps.56.184.
- [6] KALAL, M., SLEZAK, O. Overview and recent progress in SBS PCM approach to self-navigation of lasers on direct drive IFE targets. Proc. SPIE 8080, Diode-Pumped High Energy and High Power Lasers; ELI: Ultrarelativistic Laser-Matter Interactions and Petawatt Photonics; and HiPER: the European Pathway to Laser Energy, 808021 (June 09, 2011). DOI 10.1117/12.892313.
- [7] MATSUMOTO, M., NISHIMURA, T. Mersenne twister: A 623-dimensionally equidistributed uniform pseudo-random number generator. *ACM Transactions on Modeling and Computer Simulation*, Vol. 8, Num. 1, 3-30. DOI 10.1145/272991.272995.

- [8] McCracken, G., Stott, P. *Fuze - energie vesmiru*. Mlada Fronta, a.s., First edition, Prague, 2006. ISBN 80-204-1453-3
- [9] Mima, K., Tikhonchuk, V., Perlado, M. Inertial fusion experiments and theory. *Nucl. Fusion*. IOP Publishing, Vol. 51, Num. 9, 2011. DOI 10.1088/0029-5515/51/9/094004.